

# Interplay between the local information based behavioral responses and the epidemic spreading in complex networks

Can Liu,<sup>1</sup> Jia-Rong Xie,<sup>2</sup> Han-Shuang Chen,<sup>3</sup> Hai-Feng Zhang,<sup>1,4,5, a)</sup> and Ming Tang<sup>6, b)</sup>

<sup>1)</sup>*School of Mathematical Science, Anhui University, Hefei 230601, P. R. China*

<sup>2)</sup>*Department of Modern Physics, University of Science and Technology of China, Hefei 230026, China*

<sup>3)</sup>*School of Physics and Material Science, Anhui University, Hefei 230601, China*

<sup>4)</sup>*Center of Information Support & Assurance Technology, Anhui University, Hefei 230601, China*

<sup>5)</sup>*Department of Communication Engineering, North University of China, Taiyuan, Shan'xi 030051, China*

<sup>6)</sup>*Web Sciences Center, University of Electronic Science and Technology of China, Chengdu 611731, China*

(Dated: 7 September 2015)

The spreading of an infectious disease can trigger human behavior responses to the disease, which in turn plays a crucial role on the spreading of epidemic. In this study, to illustrate the impacts of the human behavioral responses, a new class of individuals,  $S^F$ , is introduced to the classical susceptible-infected-recovered ( $SIR$ ) model. In the model,  $S^F$  state represents that susceptible individuals who take self-initiate protective measures to lower the probability of being infected, and a susceptible individual may go to  $S^F$  state with a response rate when contacting an infectious neighbor. Via the percolation method, the theoretical formulas for the epidemic threshold as well as the prevalence of epidemic are derived. Our finding indicates that, with the increasing of the response rate, the epidemic threshold is enhanced and the prevalence of epidemic is reduced. The analytical results are also verified by the numerical simulations. In addition, we demonstrate that, because the mean field method neglects the dynamic correlations, a wrong result based on the mean field method is obtained—the epidemic threshold is not related to the response rate, i.e., the additional  $S^F$  state has no impact on the epidemic threshold.

PACS numbers: 89.75.-k, 87.23.Ge, 02.50.Le, 05.65.+b

Human behavioral responses to the spreading of epidemics have been recognized to have great influence on the epidemic dynamics. Therefore, it is very important to incorporate human behaviors into epidemiological models, which could improve models' utility in reflecting the reality and studying corresponding controlling measures. However, analytically-grounded approaches to the problem of interacting effect between epidemic dynamics and human behavioral responses are still lacking so far, and what can help us better understand the impacts of human behavioral responses. In this work, by introducing a new  $S^F$  state into classical  $SIR$  model to mimic the situation that, when susceptible individuals are aware of the risk of infection, they may take self-protective measures to lower the probability of being infected. We then derive theoretical formulas based on the percolation method for the epidemic threshold and the prevalence of epidemic. Our results indicate that the introduction of the new  $S^F$  state can significantly enhance the epidemic threshold and reduce the prevalence of epi-

demic. It is worth mentioning that a wrong result may be obtained when using the traditional mean field method—the epidemic threshold is not altered by the additional  $S^F$  state. The result highlights that if the effects of human behavioral responses are ignored in mathematical modeling, the obtained results cannot really reflect the spreading mechanism of epidemics among human population.

## I. INTRODUCTION

Since network models can well describe the spreading of infectious disease among populations, many efforts have been devoted to studying this field<sup>1,2</sup>. At first, researchers mainly paid attention to analyze the impact of the network structure on epidemic spreading and the control strategies, for example, how the network topology affects the epidemic threshold and the prevalence of epidemic<sup>3-8</sup>, or how to design an effective immunization strategy to control the outbreaks of epidemics<sup>9,10</sup>. In reality, outbreaks of epidemics can trigger spontaneous behavioral responses of individuals to take preventive measures, which in turn alters the epidemic dynamics and affects the disease transmission process<sup>11-17</sup>. Thus, recently, some studies have made attempts to evaluate the

<sup>a)</sup>Electronic mail: haifengzhang1978@gmail.com

<sup>b)</sup>Electronic mail: tangminghuang521@hotmail.com

impact of the human behaviors on epidemic dynamics. For instance, Funk *et al.*<sup>18</sup> studied the impacts of awareness spread on both epidemic threshold and prevalence, and they found that, in a well-mixed population, spread of awareness can reduce the prevalence of epidemic but does not tend to affect the epidemic threshold, yet the epidemic threshold is altered when considering on social networks; Sahneh *et al.* considered a Susceptible-Alter-Infected-Susceptible (*SAIS*) model<sup>19</sup>, and they found that the way of behavioral response can enhance the epidemic threshold; Meloni *et al.* constructed a meta-population model incorporating several scenarios of self-initiated behavioral changes into the mobility patterns of individuals, and they found that such behavioral changes do not alter the epidemic threshold, but may increase rather than decrease the prevalence of epidemic<sup>20</sup>. Meanwhile, in Ref.<sup>21</sup>, by designing the transmission rate of epidemic as a function of the local infected density or the global infected density, Wu *et al.* investigated the effect of such a behavioral response on the epidemic threshold.

One fact is that, the infectious neighbors can infect a susceptible individual, they can also trigger the awareness of the susceptible individual<sup>19,22</sup>. In view of this, in Ref.<sup>23</sup>, Perra *et al.* introduced a new class of individuals,  $S^F$ , that represents susceptible people who self-initiate behavioral changes that lead to a reduction in the transmissibility of the infectious disease, into the classical *SIR* model, and they found that such a model ( $SS^FIR$ ) can induce a rich phase space with multiple epidemic peaks and tipping points. However, the network structure was not incorporated into these models. As we know, when the model is considered within the network based framework, new theoretical tools should be used and new phenomena may be observed. In view of this, we incorporate the network structure into the  $SS^FIR$  model<sup>23</sup> to investigate its spreading dynamics. In the model, when contacting an infectious neighbor, susceptible individuals may be infected (from  $S$  state to  $I$  state) with a transmission rate or a behavioral response may be triggered (from  $S$  state to  $S^F$  state) with a response rate. We provide a theoretical formula for the epidemic threshold as well as the prevalence of epidemic via the percolation method<sup>5</sup>, our results show that the introduction of  $S^F$  class can enhance the epidemic threshold and reduce the prevalence of epidemic. We also demonstrate that a wrong result can be obtained—the introduction of  $S^F$  class cannot alter the epidemic threshold when using mean field method to such a model. The reasons are presented in Sec. V.

## II. DESCRIPTIONS OF THE MODEL

For the classical *SIR* model on complex network, where each node on network can be in one of three states: Susceptible ( $S$ ), Infected ( $I$ ) or Recovered ( $R$ ). The transmission rate along each  $SI$  link is  $\beta$ , and an infected node can enter  $R$  state with a recovery rate  $\mu$ . To reflect the fact that, upon observation of infection, susceptible

individuals may adopt protective measures to lower their infection risk, a new class, denoted by  $S^F$ , is introduced into the original *SIR* model, we use  $SS^FIR$  model to denote the modified *SIR* model in this study. In the model, when an  $S$  node contacts an  $I$  neighbor, besides the probability of being infected, the  $S$  node can go to  $S^F$  state with a response rate  $\beta_F \geq 0$ . The transmission rate for the  $S^F$  nodes is lower, thus we assume the transmission rate for  $S^F$  nodes is  $\gamma\beta$ , where  $0 \leq \gamma < 1$  is a discount factor.

The  $SS^FIR$  model is described by the four following reactions and the associated rates:

$$S + I \xrightarrow{\beta} 2I, \quad (1)$$

$$S + I \xrightarrow{\beta_F} S^F + I, \quad (2)$$

$$S^F + I \xrightarrow{\gamma\beta} 2I, \quad (3)$$

$$I \xrightarrow{\mu} R. \quad (4)$$

Note that the  $SS^FIR$  model returns to the *SIR* model once  $\beta_F = 0$ , and the  $S^F$  state corresponds to fully vaccinated state when  $\gamma = 0$ .

## III. THEORETICAL ANALYSIS

In our model, during a sufficiently small time interval  $\Delta t$ , the transition rates of an  $SI$  edge becoming an  $II$ ,  $S^FI$  and  $SR$  edge are  $\beta$ ,  $\beta_F$  and  $\mu$ , respectively. As a result, the probabilities of an  $SI$  edge becoming an  $II$  and  $S^FI$  edge are given as  $T_1 = \frac{\beta}{\beta + \beta_F + \mu}$  and  $T_2 = \frac{\beta_F}{\beta + \beta_F + \mu}$ , respectively. Similarly, since the transition rate of an  $S^FI$  edge becoming an  $II$  and  $S^FR$  during a sufficiently small time interval  $\Delta t$  are  $\gamma\beta$  and  $\mu$ , the probability of an  $S^FI$  edge becoming an  $II$  edge is  $T_3 = \frac{\gamma\beta}{\gamma\beta + \mu}$ .<sup>24</sup>

To analyze our proposed model, we first define “externally infected neighbor” (EIN) for any node. For node  $i$ , if a neighbor  $j$  is an EIN means that  $j$  is infected by its neighbors other than  $i$  (i.e.,  $j$  is infected even though node  $i$  is deleted from the networks, which is the basic assumption of the cavity theory in statistical physics. Note that this method is suitable for the networks with negligible number of loops as the network size is sufficiently large<sup>25</sup>). The probability of neighbor  $j$  being an EIN of  $i$  is defined as  $\theta$ , then, for the a node with degree  $k$ , the probability of having  $m$  EINs is given as:

$$p(m|k) = \binom{k}{m} \theta^m (1 - \theta)^{k-m} \quad (5)$$

Let  $p(R|m)$  be the probability of  $i$  being infected when it has number  $m$  of EIN. To calculate such a probability, we need to recognize that, in our model, an  $S$  node can become an  $I$  node through two ways: (a) the  $S$  node is directly infected; or (b) the  $S$  node first goes to  $S^F$  state and then is infected. To facilitate the analysis, we approximately assume that the impacts of  $i$ 's infected neighbors on node  $i$  happen in a non-overlapping order, i.e., they play roles on node  $i$  one by one.

For case (a), the probability of node  $i$  being infected by the  $s$ th infected neighbor is given as:

$$A_1 = (1 - T_1 - T_2)^{s-1} T_1, \quad (6)$$

Eq. (6) indicates that previous  $s - 1$  infected neighbors have not changed the state of node  $i$  (not become  $I$  or  $S^F$  state) before they become  $R$  state. Therefore, the probability of  $i$  being infected is:

$$p_1(R|m) = \sum_{s=1}^m A_1 = \frac{T_1}{T_1 + T_2} [1 - (1 - T_1 - T_2)^m]. \quad (7)$$

For case (b), node  $i$  should first become  $S^F$  state, and the probability that the susceptible node  $i$  is altered by the  $l$ th infected neighbors and becomes  $S^F$  can be written as:

$$A_2 = (1 - T_1 - T_2)^{l-1} T_2, \quad (8)$$

which also indicates that previous  $l - 1$  infected neighbors have not changed the state of node  $i$  before they become  $R$  state. For the remainder  $m - l + 1$  infected neighbors (including the infected neighbor who just made  $i$  go to  $S^F$  state), they can infect  $i$  with probability:

$$A_3 = 1 - (1 - T_3)^{m-l+1}. \quad (9)$$

As a result, the probability of node  $i$  first becoming  $S^F$  state and then going to  $I$  state is:

$$p_2(R|m) = \sum_{l=1}^m A_2 * A_3 = \frac{T_2}{T_1 + T_2} [1 - (1 - T_1 - T_2)^m] - \frac{(1 - T_3)T_2}{T_1 + T_2 - T_3} [(1 - T_3)^m - (1 - T_1 - T_2)^m]. \quad (10)$$

The probability  $p(R|m)$  is

$$\begin{aligned} p(R|m) &= p_1(R|m) + p_2(R|m) = 1 - (1 - T_1 - T_2)^m \\ &\quad - \frac{(1 - T_3)T_2}{T_1 + T_2 - T_3} [(1 - T_3)^m - (1 - T_1 - T_2)^m] \\ &= 1 - \frac{T_1 - T_3 + T_2 T_3}{T_1 + T_2 - T_3} (1 - T_1 - T_2)^m \\ &\quad - \frac{(1 - T_3)T_2}{T_1 + T_2 - T_3} (1 - T_3)^m. \end{aligned} \quad (11)$$

Combing Eqs. (5) and (11), the probability of a node

with degree  $k$  being infected is

$$\begin{aligned} p(R|k) &= \sum_m p(R|m) p(m|k) = 1 - (1 - \theta T_1 - \theta T_2)^k \\ &\quad - \frac{(1 - T_3)T_2}{T_1 + T_2 - T_3} [(1 - \theta T_3)^k - (1 - \theta T_1 - \theta T_2)^k] \\ &= 1 - \frac{T_1 - T_3 + T_2 T_3}{T_1 + T_2 - T_3} (1 - \theta T_1 - \theta T_2)^k \\ &\quad - \frac{(1 - T_3)T_2}{T_1 + T_2 - T_3} (1 - \theta T_3)^k. \end{aligned} \quad (12)$$

Then the EIN probability  $\theta$  is the solution to the self-consistent condition

$$\begin{aligned} \theta &= \sum_k Q(k) p(R|k) \\ &= 1 - \frac{T_1 - T_3 + T_2 T_3}{T_1 + T_2 - T_3} G_1(1 - \theta T_1 - \theta T_2) \\ &\quad - \frac{(1 - T_3)T_2}{T_1 + T_2 - T_3} G_1(1 - \theta T_3) = f(\theta). \end{aligned} \quad (13)$$

In Eq. (13),  $Q(k) = \frac{(k+1)P(k+1)}{\langle k \rangle}$  is the excess degree distribution, where  $P(k)$  is the degree distribution and  $\langle k \rangle$  is the average degree. The generating function for  $Q(k)$  is given as

$$G_1(x) = \sum_{k=0} Q(k) x^k. \quad (14)$$

There is a trivial solution  $\theta = 0$  in self-consistent equation (13). To have a non-trivial solution, the following condition must be met:

$$\left. \frac{df(\theta)}{d\theta} \right|_{\theta=0} = (T_1 + T_2 T_3) G_1'(1) \geq 1, \quad (15)$$

which implies the epidemic can outbreak when

$$\frac{\beta}{\mu + \gamma\beta} \frac{\mu + \gamma\beta + \gamma\beta_F}{\mu + \beta + \beta_F} \geq \frac{\langle k \rangle}{\langle k^2 \rangle - \langle k \rangle}. \quad (16)$$

For the prevalence of epidemic (defined as  $R(\infty)$ ), we can numerically solve  $\theta$  from self-consistent equation (13), then the formula of  $R(\infty)$  is

$$\begin{aligned} R(\infty) &= \sum_k P(k) p(R|k) \\ &= 1 - \frac{T_1 - T_3 + T_2 T_3}{T_1 + T_2 - T_3} G_0(1 - \theta T_1 - \theta T_2) \\ &\quad - \frac{(1 - T_3)T_2}{T_1 + T_2 - T_3} G_0(1 - \theta T_3). \end{aligned} \quad (17)$$

In Eq. (17),  $G_0(\cdot)$  is the generating function of degree distribution  $P(k)$ , which is described as:

$$G_0(x) = \sum_{k=0} P(k) x^k. \quad (18)$$

#### IV. SIMULATION RESULTS

In this section, we perform an extensive set of Monte Carlo simulations to validate the theoretical predictions in Section III. Here we carry out simulations on an Erdős-Rényi network (labeled ER network)<sup>26</sup> with network size  $N = 10000$  and average degree  $\langle k \rangle = 10$ , and a configuration network generated by an uncorrelated configuration model (UCM)<sup>27</sup>. The configuration network also has  $N = 10000$  nodes and the degree distribution meets  $P(k) \sim k^{-3.0}$ , whose minimal and maximal degrees are  $k_{min} = 3$  and  $k_{max} = \sqrt{N}$ , respectively.

##### A. Results on ER network

Differing from the *SIS* (Susceptible-Infected-Susceptible) model, it is not an easy thing to determine the epidemic threshold for the *SIR* model owing to the non-zero value of  $R$ . In doing so, in Ref.<sup>28</sup>, Shu et al. suggested that the variability measure

$$\Delta = \frac{\sqrt{\langle \rho^2 \rangle - \langle \rho \rangle^2}}{\langle \rho \rangle} \quad (19)$$

can well predict the epidemic threshold for the *SIR* model, where  $\rho$  denotes the prevalence of epidemic in one simulation realization<sup>29,30</sup>.  $\Delta$  can be explained as the standard deviation of the epidemic prevalence, and is a standard measure to determine critical point in equilibrium phase on magnetic system<sup>31</sup>. In our simulations, we have taken at least 1000 independent realizations to predict the epidemic threshold. For convenience, in this study, we set recovery rate  $\mu = 1.0$ .

In Fig. 1, for different response rate  $\beta_F$ , the value of  $R(\infty)$  (upper panels) and the measure  $\Delta$  (lower panels) as the functions of the transmission rate  $\beta$  are investigated. As shown in Fig. 1, one can observe that the variability measure can well predict the epidemic threshold for our *SS<sup>F</sup>IR* model. As a result, in the following figures, we use this method to determine the epidemic threshold, i.e., the point where the value of  $\Delta$  is the maximal. Fig. 1 also describes that, no matter  $\gamma = 0.1$  [see Figs. 1(a)-(b)] or  $\gamma = 0.3$  [see Figs. 1(c)-(d)], on the one hand, the epidemic threshold is enhanced as the response rate  $\beta_F$  is increased. On the other hand, for the a fixed value of  $\beta$ , Figs. 1(a) and (c) suggest that the prevalence of epidemic is remarkably reduced when  $\beta_F$  is increased. The results suggest that, by introducing an additional protective state,  $S^F$ , to the classical *SIR* model, the conclusions are quite different from the previous results which have not incorporated the impacts of human behavioral responses. The result again emphasizes the fact that the spontaneous behavioral responses of individuals to the emergent diseases have vital impacts on the epidemic dynamics. If the behavioral responses are ignored in mathematical modelling, the obtained results cannot really reflect the spreading mechanism of epidemics among human population.

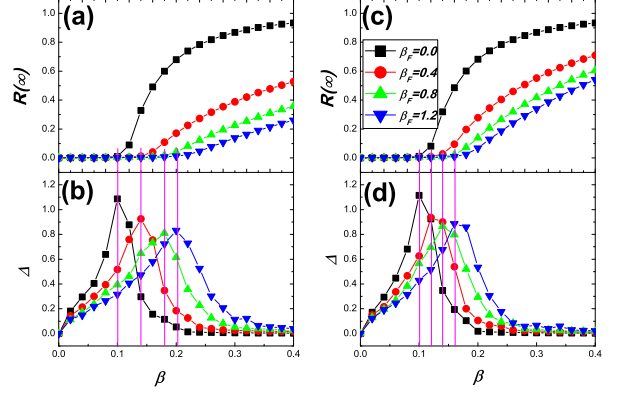


FIG. 1. (Color online) On ER networks, the prevalence of epidemic  $R(\infty)$  (upper panels) and the variability measure  $\Delta$  (lower panels) as functions of the transmission rate  $\beta$  for different values of  $\beta_F$  and  $\gamma$ . Note that, here  $\beta_F$  is a rate rather probability, as a result, whose value may be larger than one. (a)-(b)  $\gamma = 0.1$ ; (c)-(d)  $\gamma = 0.3$ . The pink lines are given to demonstrate that the peak value of  $\Delta$  corresponds to the epidemic threshold  $\beta_c$ .

We then compare the theoretical results with the Monte Carlo simulations on ER network in Fig. 2 and Fig. 3. Since the degree distribution of an Erdős-Rényi network is  $P(k) = e^{-\langle k \rangle} \frac{\langle k \rangle^k}{k!}$ , the generating functions meet:

$$G_0(x) = G_1(x) = e^{\langle k \rangle(x-1)} \quad (20)$$

According to Ineq. (15), the epidemic threshold  $\beta_c$  for ER network is determined by the following equation

$$\frac{\beta_c}{\mu + \gamma\beta_c} \frac{\mu + \gamma\beta_c + \gamma\beta_F}{\mu + \beta_c + \beta_F} = \frac{1}{\langle k \rangle}. \quad (21)$$

Moreover, substituting Eq. (20) into Eq. (13) and Eq. (17), the prevalence of epidemic  $R(\infty)$  can be easily solved.

The comparison of  $R(\infty)$  between the simulations and the theoretical result is plotted in Fig. 2, which indicates that the numerical simulation and the theoretical result are in good agreement. Meanwhile, the epidemic threshold for  $\beta_c$  obtained from Eq. (21) and from numerical method (i.e., the point where  $\Delta$  is maximal) is compared in Fig. 3, which also indicates that the epidemic threshold predicated by our method is remarkable agreement with numerical simulations. The result in Fig. 3 also suggests that the epidemic threshold  $\beta_c$  is increased as the value of  $\gamma$  is decreased. Importantly, the reduction is more efficient when the response rate  $\beta_F$  is larger.

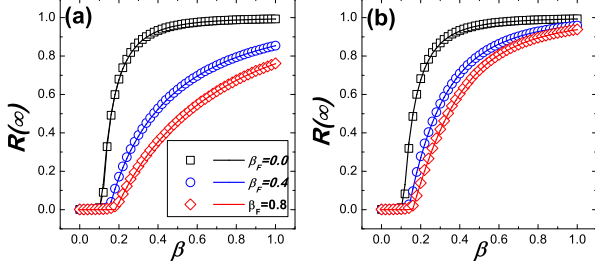


FIG. 2. (Color online) Comparison between the Monte Carlo based simulations and the theoretical predictions for  $R(\infty)$  on ER networks. The simulation results are denoted by symbols and the theoretical predictions are denoted by the corresponding lines. The theoretical results are obtained by substituting Eq. (20) into Eqs. (13) and (17), and the value of  $\theta$  is numerically solved from Eq. (13), then  $R(\infty)$  is got from Eq. (17). (a)  $\gamma = 0.1$ ; (b)  $\gamma = 0.3$ .

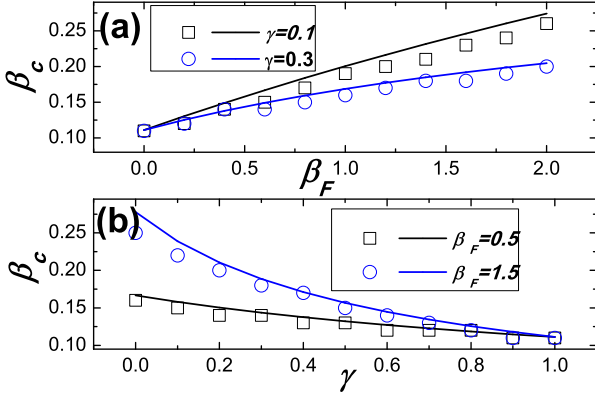


FIG. 3. (Color online) Comparison between the Monte Carlo based simulations and the theoretical predictions for the epidemic threshold  $\beta_c$  on ER networks. The theoretical predictions denoted by lines are obtained from Eq. (21), and the simulation results denoted by symbols are the points where the values  $\Delta$  are maximal. (a)  $\beta_c$  as a function of the response rate  $\beta_F$  for different values of  $\gamma$ ; (b)  $\beta_c$  as a function of the discount factor  $\gamma$  for different values of  $\beta_F$ .

## B. Results on UCM network

Real complex networked systems often possess certain degree of skewness in their degree distributions, typically represented by some scale-free topology. We thus check our model on UCM network with degree distribution  $P(k) \sim k^{-3.0}$  to illustrate that our theory can generalize to the networks with heterogenous degree distribution and in the absence of degree-to-degree correlation.

As shown in Fig. 4 and Fig. 5, one can see that the analytical results are in good agreement with the numerics.

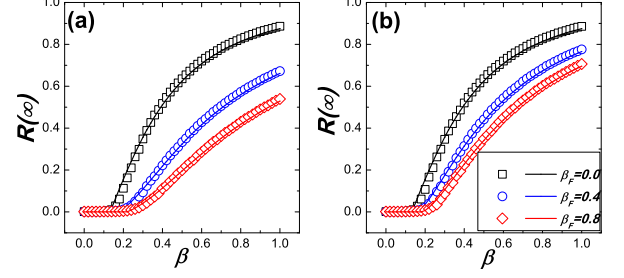


FIG. 4. (Color online) Comparison between the Monte Carlo based simulations and the theoretical predictions for  $R(\infty)$  on UCM networks. The simulation results are denoted by symbols and the theoretical predictions are denoted by the corresponding lines. The theoretical results are obtained by substituting a fixed degree distribution  $P(k)$  into Eqs. (18) and (18), and then  $R(\infty)$  can be solved from Eqs. (18) and (18) as described in Fig. 2. (a)  $\gamma = 0.1$ ; (b)  $\gamma = 0.3$ .

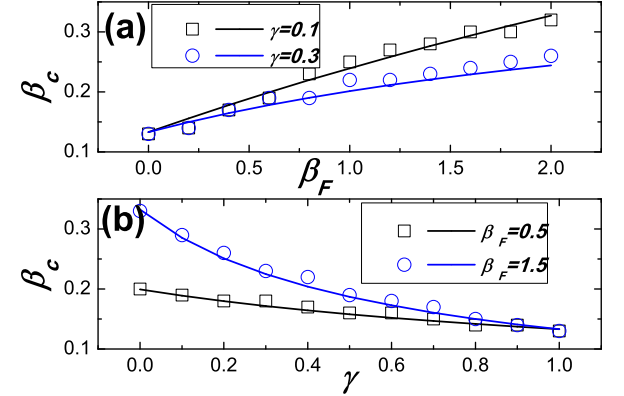


FIG. 5. (Color online) Comparison between the Monte Carlo based simulations and the theoretical predictions for the epidemic threshold  $\beta_c$  on UCM networks. The theoretical predictions denoted by lines are obtained from Ineq. (16), and the simulation results denoted by symbols are the points where the values  $\Delta$  are maximal. (a)  $\beta_c$  as a function of the response rate  $\beta_F$  for different values of  $\gamma$ ; (b)  $\beta_c$  as a function of the discount factor  $\gamma$  for different values of  $\beta_F$ .

They also indicate that, since increasing  $\beta_F$  can induce more susceptible individuals go to  $S^F$  state and reducing  $\gamma$  can lower the risk of  $S^F$  nodes, as a result, both of them can lower the prevalence of epidemic  $R(\infty)$  and increase the epidemic threshold  $\beta_c$ .

## V. MEAN FIELD METHOD FOR THE MODEL

One possible way to describe our proposed  $SS^FIR$  model is the mean field method, which can be written



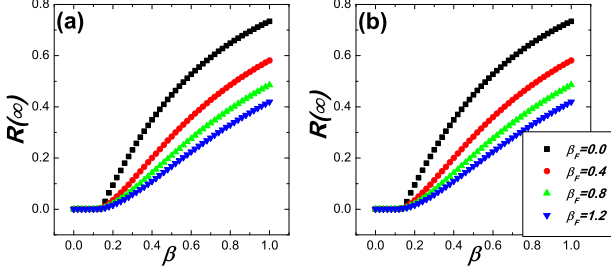


FIG. 6. (Color online) Based on the differential Eqs. (22)-(23), the prevalence of epidemic  $R(\infty)$  as a function of  $\beta$  is presented. (a)  $\gamma = 0.1$ ; (b)  $\gamma = 0.3$ .

as:

$$\frac{dS_k(t)}{dt} = -\beta k S_k \Theta - \beta_F k S_k \Theta, \quad (22)$$

$$\frac{dS_k^F(t)}{dt} = \beta_F k S_k \Theta - \beta \gamma k S_k^F \Theta, \quad (23)$$

$$\frac{dI_k(t)}{dt} = k \Theta \beta (S_k + \gamma S_k^F) - I_k, \quad (24)$$

$$\frac{dR_k(t)}{dt} = I_k, \quad (25)$$

where the factor  $\Theta(t) = \sum_{k'} P(k'|k) I_{k'}(t)$  represents the probability that any given link points to an infected node. In absence of any degree correlations,  $\Theta(t) = \frac{1}{\langle k \rangle} \sum_k k P(k) I_k(t)$ <sup>32</sup>.

Based on the above differential equations, we can obtain that the epidemic threshold  $\beta_c = \frac{\langle k \rangle}{\langle k^2 \rangle}$  (detailed derivation is given in section VII), which means that the epidemic threshold for our model is not related to the response rate  $\beta_F$  or the discount factor  $\gamma$ , and which is the same to the epidemic threshold of classical *SIR* model. The simulation results based on the Eqs. (22-25) in Fig. 6 also indicate that, based on mean field method, the epidemic threshold is not altered by different values of  $\beta_F$  or  $\gamma$ . However, our previous simulation results based on Monte Carlo method have suggested that the epidemic threshold  $\beta_c$  is increased when  $\beta_F$  is increased or  $\gamma$  is reduced. That is to say, the conclusion obtained by mean-field method is wrong.

Now let us explain why the mean field method gives a wrong result. It is known that, near the epidemic threshold, the fraction of infected nodes (label  $\rho_I$ ) is very small. When using the mean field method, the dynamic correlation is neglected, the probability of  $S$  node becoming  $S^F$  is proportional to  $O(\rho_I)$  since the average fraction of infected nodes among neighborhood equals to  $O(\rho_I)$ . Similarly, the probability of  $S^F$  node becoming  $I$  node is also proportional to  $O(\rho_I)$ . As a result, the probability of  $S \rightarrow S^F \rightarrow I$  is proportional to  $O(\rho_I^2)$ , which leads to the effect of the  $S^F$  is ignored and the epidemic threshold obtained by the mean field method is not related to the value of  $\beta_F$  or  $\gamma$ . In fact, when an  $S$  node becomes

an  $S^F$  node there must exist at least one infected nodes among the neighborhood of the  $S$  node. More importantly, these infected neighbors may exist for a certain time interval, so the probability of  $S \rightarrow S^F \rightarrow I$  is not proportional to  $O(\rho_I^2)$ . However, as deduced in Eq. (9), the dynamics correlation near the epidemic threshold is considered in our above analysis, which can accurately predict the epidemic threshold.

## VI. CONCLUSIONS

To summarize, we have proposed an *SS<sup>F</sup>IR* epidemiological model in complex networks, in which the probability of susceptible individuals becoming  $S^F$  state is proportional to the number of infected neighbors, to reflect the fact that individuals are more likely to take protective measures when they find their neighbors are infected. By using theoretical analysis as well as numerical simulations, we found that the prevalence of epidemic is effectively reduced and the epidemic threshold is remarkably increased when the response rate  $\beta_F$  is increased or the discount factor  $\gamma$  is reduced. Moreover, we have demonstrated that the mean field based analysis provides a wrong result: the epidemic threshold is not related to the response rate  $\beta_F$  or discount factor  $\gamma$ . The reason is that, near the epidemic threshold, the probability of  $S \rightarrow S^F \rightarrow I$  is a second order infinitesimal since the mean field method ignores the dynamic correlation, which makes the effect of  $S^F$  state to be ignored.

With the development of technology, information induced awareness or self-protective behaviors can not only diffuse through the contact networks where the diseases spread but also can fast diffuse through many different channels, such as, the word of mouth, news media, online social networks, and so on. In view of this, recent well-studied multiplex network theory may be an ideal framework to mimic the interplay of information or related awareness and the epidemic dynamics<sup>33-35</sup>. Thus, how to generalize our model to multiplex networks and provide theoretical analysis to the model is a challenge in our further work.

## VII. APPENDIX

When assuming  $S_k(0) \approx 1$ , then from Eq. (22), we have<sup>32</sup>

$$S_k(t) = e^{-k(\beta + \beta_F)\phi(t)}, \quad (26)$$

where  $\phi(t) = \int_0^t \Theta(t') dt' = \frac{1}{\langle k \rangle} \sum_k k P(k) R_k(t)$ .

Substituting Eq. (26) into Eq. (23), one has:

$$\frac{dS_k^F}{dt} = \beta_F k \Theta(t) e^{-k(\beta + \beta_F)\phi(t)} - \beta \gamma k S_k^F \Theta(t). \quad (27)$$

By using the variation of constants method,  $S_k^F(t)$  is

solved as:

$$S_k^F(t) = \frac{\beta_F}{\beta + \beta_F - \beta\gamma} e^{-\beta\gamma k\phi(t)} (1 - e^{-k(\beta + \beta_F - \beta\gamma)\phi(t)}). \quad (28)$$

Then,

$$\begin{aligned} \Theta(t) &= \frac{d\phi(t)}{dt} = 1 - \phi(t) - \frac{1}{\langle k \rangle} \Sigma k P(k) e^{-k(\beta + \beta_F)\phi(t)} \\ &\quad - \frac{1}{\langle k \rangle} \Sigma k P(k) \frac{\beta_F}{\beta + \beta_F - \beta\gamma} e^{-\beta\gamma k\phi(t)} (1 - e^{-k(\beta + \beta_F - \beta\gamma)\phi(t)}). \end{aligned} \quad (29)$$

By letting  $\phi_\infty = \lim_{t \rightarrow \infty} \phi(t)$ , and with the fact that

$\lim_{t \rightarrow \infty} \frac{d\phi(t)}{dt} = 0$  and  $I(t \rightarrow \infty) = 0$  when the epidemics end, a self-consistent equation can be got from Eq. (29):

$$\begin{aligned} \phi_\infty &= 1 - \frac{1}{\langle k \rangle} \Sigma k P(k) e^{-k(\beta + \beta_F)\phi_\infty} \\ &\quad - \frac{1}{\langle k \rangle} \Sigma k P(k) \frac{\beta_F}{\beta + \beta_F - \beta\gamma} e^{-\beta\gamma k\phi_\infty} (1 - e^{-k(\beta + \beta_F - \beta\gamma)\phi_\infty}) = g(\phi_\infty). \end{aligned} \quad (30)$$

The value  $\phi_\infty = 0$  is always a solution. In order to have a non-zero solution, the condition

$$\begin{aligned} \left. \frac{df(\phi_\infty)}{d\phi_\infty} \right|_{\phi_\infty=0} &= \frac{(\beta + \beta_F)\langle k^2 \rangle}{\langle k \rangle} - \frac{\beta_F \langle k^2 \rangle}{\langle k \rangle} \\ &= \frac{\beta \langle k^2 \rangle}{\langle k \rangle} \geq 1 \end{aligned} \quad (31)$$

should be satisfied, which means that the epidemic threshold  $\beta_c = \frac{\langle k \rangle}{\langle k^2 \rangle}$ .

## ACKNOWLEDGMENTS

This work is funded by the National Natural Science Foundation of China (Grant Nos. 61473001, 91324002, 11331009).

- <sup>1</sup>M. E. J. Newman, SIAM review **45**, 167 (2003).
- <sup>2</sup>M. E. J. Newman, *Networks: an introduction* (Oxford University Press, 2010).
- <sup>3</sup>M. Barthélemy, A. Barrat, R. Pastor-Satorras, and A. Vespignani, Journal of Theoretical Biology **235**, 275 (2005).
- <sup>4</sup>C. Castellano and R. Pastor-Satorras, Physical Review Letters **105**, 218701 (2010).
- <sup>5</sup>M. E. J. Newman, Physical Review E **66**, 016128 (2002).
- <sup>6</sup>P. Holme and T. Takaguchi, Phys. Rev. E **91**, 042811 (2015).
- <sup>7</sup>R. Pastor-Satorras and A. Vespignani, Physical Review Letters **86**, 3200 (2001).
- <sup>8</sup>P. Holme, PLoS ONE **8**, e84429 (2013).
- <sup>9</sup>R. Pastor-Satorras and A. Vespignani, Physical Review E **65**, 036104 (2002).
- <sup>10</sup>R. Cohen, S. Havlin, and D. Ben-Avraham, Physical Review Letters **91**, 247901 (2003).

- <sup>11</sup>H.-F. Zhang, Z. Yang, Z.-X. Wu, B.-H. Wang, and T. Zhou, Scientific Reports **3**, 3292 (2013).
- <sup>12</sup>Z. Ruan, M. Tang, and Z. Liu, Phys. Rev. E **86**, 036117 (2012).
- <sup>13</sup>C. T. Bauch, A. P. Galvani, and D. J. Earn, Proceedings of the National Academy of Sciences **100**, 10564 (2003).
- <sup>14</sup>C. T. Bauch and D. J. Earn, Proceedings of the National Academy of Sciences of the United States of America **101**, 13391 (2004).
- <sup>15</sup>L. Wang, Y. Zhang, T. Huang, and X. Li, Physical Review E **86**, 032901 (2012).
- <sup>16</sup>S. Funk, M. Salathé, and V. A. Jansen, Journal of The Royal Society Interface **7**, 1247 (2010).
- <sup>17</sup>X.-T. Liu, Z.-X. Wu, and L. Zhang, Physical Review E **86**, 051132 (2012).
- <sup>18</sup>S. Funk, E. Gilad, C. Watkins, and V. A. Jansen, Proceedings of the National Academy of Sciences **106**, 6872 (2009).
- <sup>19</sup>F. D. Sahneh, F. N. Chowdhury, and C. M. Scoglio, Scientific Reports **2**, 632 (2012).
- <sup>20</sup>S. Meloni, N. Perra, A. Arenas, S. Gómez, Y. Moreno, and A. Vespignani, Scientific Reports **1**, 62 (2011).
- <sup>21</sup>Q. Wu, X. Fu, M. Small, and X.-J. Xu, Chaos **22**, 013101 (2012).
- <sup>22</sup>H.-F. Zhang, J.-R. Xie, M. Tang, and Y.-C. Lai, Chaos **24**, 043106 (2014).
- <sup>23</sup>N. Perra, D. Balcan, B. Gonçalves, and A. Vespignani, PLoS ONE **6**, e23084 (2011).
- <sup>24</sup>L. Hébert-Dufresne, O. Patterson-Lomba, G. M. Goerg, and B. M. Althouse, Physical Review Letters **110**, 108103 (2013).
- <sup>25</sup>M. E. J. Newman and C. R. Ferrario, PLoS ONE **8**, e71321 (2013).
- <sup>26</sup>P. Erdős and A. Rényi, Publ. Math. Inst. Hungar. Acad. Sci **5**, 17 (1960).
- <sup>27</sup>M. E. J. Newman, S. H. Strogatz, and D. J. Watts, Physical Review E **64**, 026118 (2001).
- <sup>28</sup>P. Shu, W. Wang, and M. Tang, arXiv preprint arXiv:1410.0459 (2014).
- <sup>29</sup>P. Crepey, F. P. Alvarez, and M. Barthélemy, Physical Review E **73**, 046131 (2006).
- <sup>30</sup>P. Shu, M. Tang, K. Gong, and Y. Liu, Chaos **22**, 043124 (2012).

- <sup>31</sup>S. C. Ferreira, R. S. Ferreira, C. Castellano, and R. Pastor-Satorras, *Physical Review E* **84**, 066102 (2011).
- <sup>32</sup>Y. Moreno, R. Pastor-Satorras, and A. Vespignani, *The European Physical Journal B* **26**, 521 (2002).
- <sup>33</sup>C. Granell, S. Gomez, and A. Arenas, *Physical Review Letters* **111**, 128701 (2013).
- <sup>34</sup>W. Wang, M. Tang, H. Yang, Y. Do, Y.-C. Lai, and G. Lee, *Scientific Reports* **4**, 5097 (2014).
- <sup>35</sup>S. Boccaletti, G. Bianconi, R. Criado, C. Del Genio, J. Gómez-Gardeñes, M. Romance, I. Sendiña-Nadal, Z. Wang, and M. Zanin, *Physics Reports* **544**, 1 (2014).